Towards 3D Virtual Histology of melanoma tissue by means of lab-based X-ray Phase Contrast Computed Micro-Tomography

G. Saccomano[1,2], L. Brombal[3], D. Dreossi[2], M. Pinamonti[4], G. Tromba[2] and F. Brun[1]

[1] *Department of Engineering and Architecture, University of Trieste, Trieste*

[2] *Elettra-Sincrotrone Trieste S.C.p.A., Trieste*

[3] *Department of Physics, University of Trieste, Trieste*

[4] *Department of Pathology, Cattinara Hospital, Trieste*

***Abstract*—Melanoma is a serious form of skin cancer which originates from melanocytes. The diagnosis of melanoma occurs through histological examination, which is a destructive and labor-intensive technique where a "blind" sectioning without landmarks is performed.**

X-ray phase contrast computed micro-tomography (micro-CT) overcomes these limitations by providing virtual sections of the excised tissue along arbitrary planes without causing its destruction. However, up to date, synchrotron radiation (SR) micro-CT seems to be the only way to obtain high-resolution phase contrast 3D data. In sight of introducing x-ray virtual histology in the clinical practice, compact laboratory x-ray phase contrast micro-CT solutions are needed.

This study aims to move towards a new concept of 3D x-ray virtual histology in the clinical trial of melanoma diagnosis by showing preliminary results from a compact and cheap lab-based micro-CT setup based on the edge-illumination principle. A thorough comparison of SR micro-CT against laboratory micro-CT of the very same melanoma tissue is presented and discussed. Conventional histological images are also included.

Although the achieved spatial resolution and the scanning speed are not comparable to those obtained with SR, the proposed lab-based micro-CT solution still provides a comprehensive understanding of the morphological and functional aspects of the melanoma tissue in a non-destructive way, thus justifying further destructive exams such as conventional histology. This lays promising foundations for a wider clinical translation of the proposed approach.

***Keywords*— Melanoma, x-ray Virtual Histology, synchrotron radiation Computed micro-Tomography, lab-based Computed micro-Tomography.**

I. Introduction

DESPITE advances made over the past decades, melanoma remains the most aggressive type of skin cancer due to its aggressive nature of rapidly spreading to other organs and becoming metastatic. Even though it accounts for only 5% of all skin cancer, it is responsible for the majority of deaths in this category [1].

Melanoma develops when DNA damage from burning or tanning due to UV radiation changes and mutates in the melanocytes, which are the cells in the upper layer of the skin that produce a pigment known as melanin, resulting in uncontrolled cellular growth. The skin phenotype plays an important role with higher risk for fair-skinned persons: in 2006 American Caucasians accounted for 70% of melanoma cases [2], while black population had an increased mortality as a results of late detection and a different biology [3].

First melanoma signs are often associated with a change in an existing mole and the development of a new pigmented or unusual-looking growth on the skin. The detection of melanoma is based on the revised ABCDE rule of pigmented lesions (Asymmetry, irregular Border, change in Color, Diameter, Evolution): when one or more of the features listed above are identified in a mole, biopsy material is removed and analysed in laboratory. Although non-invasive in-vivo approaches such as e.g., optoacoustic and ultrasonography techniques [4] have been proposed, histological examination of bioptic material is still the standard for diagnosis of pathological tissues, mainly based on cancer cells recognition and diffusion in the excised tissue which can occur also at higher penetration depths. However, the histological staining process is based on a complex and time-consuming chemical preparation of the excised biopsy, followed by sectioning the pathological tissue into thin slices for viewing under the light microscope.

To overcome the lack of reproducibility and destructiveness of the histological technique, x-ray Virtual Histology (xVH) exploits x-ray Computed micro-Tomography (micro-CT) in the production of 3D high-contrast maps of the soft tissue specimen. By virtually sectioning the whole excised sample, xVH allows to investigate structures (e.g., lesions) and computing parameters (e.g., max infiltration depth) that could be lost or damaged during the histological sectioning process.

Synchrotron Radiation Computed micro-Tomography (SR micro-CT) is the optimum technique in term of high-resolution and high-contrast properties for xVH. However, it lacks the possibility of an easy integration in the clinical workflow due to its limited-access policy and high cost of maintenance.

This work aims to show the potentiality of a lab-based phase-contrast micro-CT technique to perform xVH on a soft tissue suspected-melanoma biopsy. As a preliminary result, we focus on enhancing the contrast-to-noise ratio by working on two aspects: a physical property (edge illumination principle) and a computational method (denoising with deep learning). SR micro-CT and histology images are considered in this study.

II. Material and Methods

A. Staining and embedding

One surgical excision of a human suspected melanoma tissue was embedded in paraffin (standard histology paraffin block of about 2.5x3.5x1.0 cm^3) and then sectioned using a microtome. The resultant skin tissue remains inside the paraffin block for micro-CT analysis.

B. Histological examination

Paraffin embedded melanoma sections were stained with haematoxylin & eosin (HE). Histological images were acquired using a D-Sight 2.0 digital microscope with a 200× magnification.

C. Lab-based Computed micro-Tomography

The paraffin block including the melanoma specimen was investigated by means of x-ray phase-contrast micro-CT at PEPILab [5] (Fig. 1). The acquisition was performed with a Hamamatsu microfocus x-ray source (tube voltage: 50kV, tube current: 120µA) and a Pixirad-1/Pixie-III detector [6]. The sample and the detector were placed respectively 355 mm and 635 mm far from the x-ray source. Two structured absorbing masks (M1: sample mask, M2: detector mask) were introduced in the micro-CT setup to exploit the edge illumination principle: the source-to-M1 distance and the sample-to-M2 distance were 315 mm and 255 mm. The mask aperture was 10 µm wide and the mask pitch was 61 µm. The pixel size obtained was 12 µm. Five points were sampled over the illumination curve and 6 dithering steps were considered. A total of 720 projections were acquired over a 360 degrees rotation of the sample with an exposure time of 3000 ms per projection.

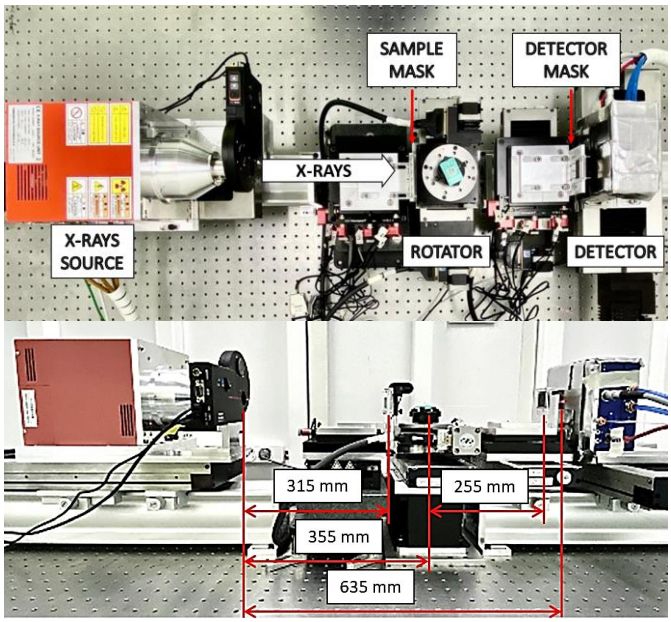

Fig. 1: Compact phase contrast micro-CT setup at PEPILab.

After being processed for phase retrieval, the stack of projections was split into 4 sets of projections and each set was reconstructed using TIGRE Toolbox [7]. Noise2Inverse denoising method [8] was applied by considering each set of reconstructed slices to get the final reconstructed volume. The Mixed-Scale Dense (MSD) convolutional neural network was used.

D. Synchrotron Radiation Computed micro-Tomography

The very same human melanoma excision was scanned at SYRMEP beamline [9] of Elettra synchrotron facility. The 2.4 GeV storage ring operating mode flux was filtered with a 1.0 mm Si filter to obtain an x-ray average energy spectrum of 23.6 keV. The pixel size was set to 1.6 µm and the sample-to-detector distance was set at 150 mm to improve the contrast-to-noise ratio by exploiting the propagation-based principle [10]. The paraffin block was placed orthogonally between the x-ray source and the detector (a Hamamatsu ORCA-FLASH 4.0 Digital CMOS camera coupled to a 17 µm GGG scintillator). 1800 projections over a 180 degrees sample rotation were collected with an exposure time of 100 ms per projection.

Projection digital images were filtered with a phase retrieval algorithm [11] and a δ/β ratio of 150. Tomographic axial slices were reconstructed using SYRMEP Tomo Project software [12] and, since two vertical scans were acquired to cover the whole mole, the two stacks were registered and stitched together with a Python script.

E. Quantitative image analysis

In order to compare the results obtained with two phase-contrast based micro-CT techniques, a quantitative evaluation was performed by computing the contrast-to-noise ratio (CNR). As shown with different colours in Fig. 2, several 20x20 pixels region-of-interests (ROIs) were considered to estimate the detectability of skin layers (epidermis, dermis, and subcutaneous fat) and pathological elements (lesion and ulceration), while confronted to the background (BKG). ROIs in Fig. 2 appear having different size due to different image pixel size (12 µm and 1.6 µm, respectively). CNR was computed as in Eq. (1):

$$CNR = \frac{|\mu_{ROI} - \mu_{BKG}|}{\sqrt{\frac{1}{2}(\sigma_{ROI}^2 + \sigma_{BKG}^2)}} \quad (1)$$

where μ is the mean and σ is the standard deviation of the gray levels within the ROI.

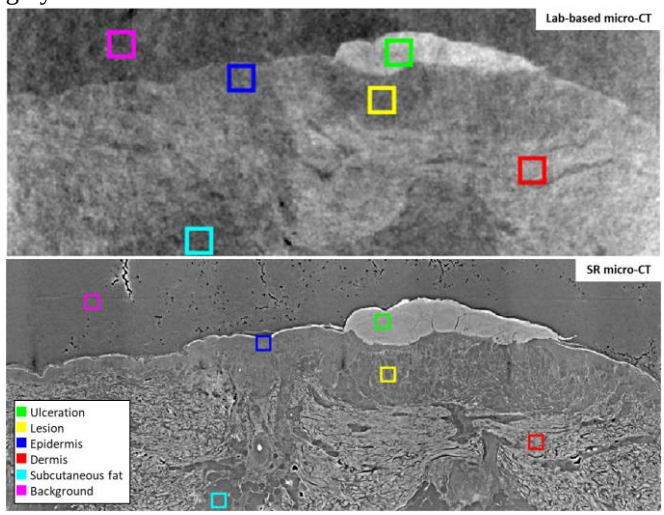

Fig. 2: Highlighted ROIs in micro-CT images used for quantitative analysis: each color marks a specific element of the skin tissue, while magenta is used as reference (background).

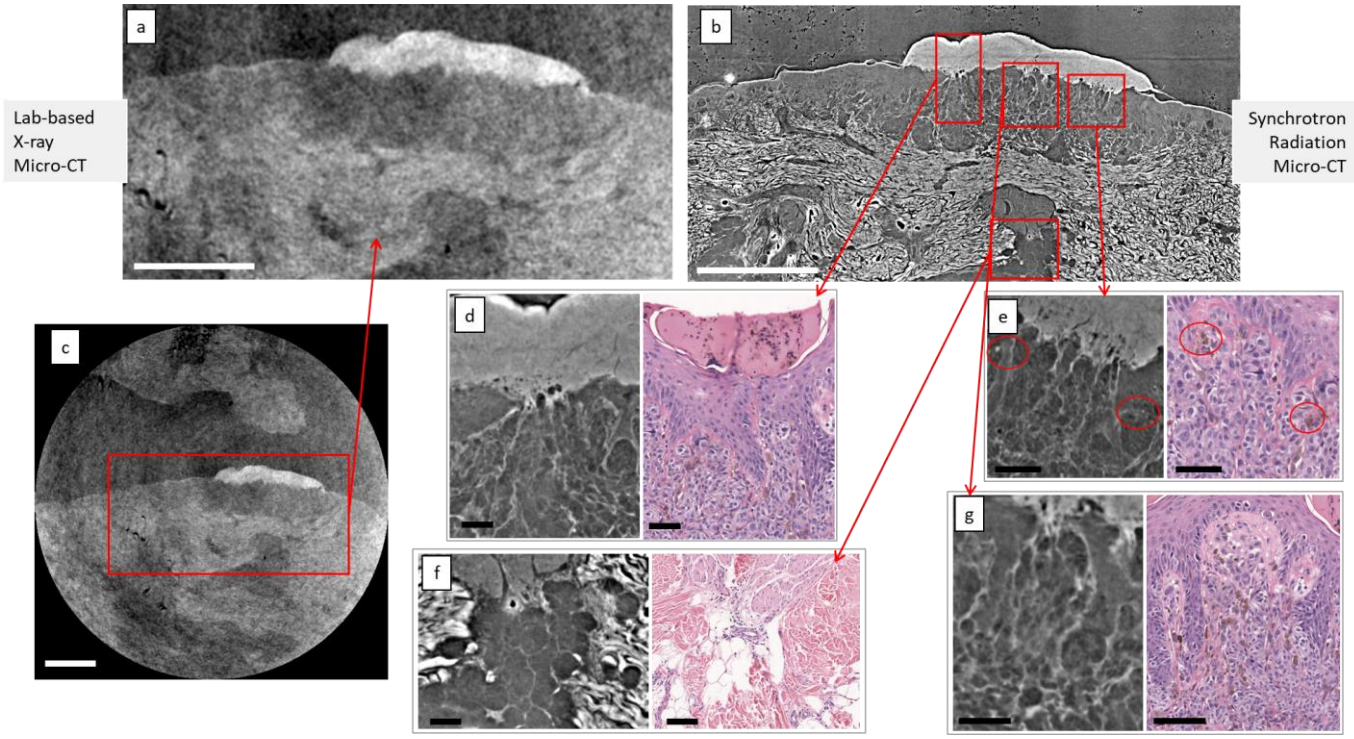

Fig. 3: The same lesion area of melanoma with (a) the lab-based and (b) the SR micro-CT techniques. (c) A lab-based micro-CT slice of the whole excision. Selected SR micro-CT and histology matches: (d) the full-thickness loss of the epidermis, (e) melanin pigment in malignant melanocytes nests, (f) dermis and subcutaneous fat and (g) the presence of malignant melanocytes in epidermis and dermis. White scale bar = 1mm, Black scale bar = 100µm.

III. Results And Discussion

From the whole 3D reconstructed datasets of micro-CT techniques¸ two slices were extracted and matched together via visual inspection. These slices are reported in Fig. 3.a and Fig. 3.b.

A. X-ray virtual histology with lab-based micro-CT

As visible for Fig. 3.c, the first aspect to consider is the challenging discrimination of the soft tissue from the paraffin due to the high density and internal artefacts introduced by the paraffin.

The application of the adopted phase retrieval to the edge-illumination technique revealed boundaries of the skin structure, thus allowing the identification of the top two layers, i.e. the epidermis and dermis (Fig. 3.a). The hypodermis, which is mainly composed by subcutaneous fat and blood vessels, is not properly observable due to its low density. Even the distinction between epidermis and dermis is not well defined with this technique, but it is an unnecessary information when finalizing the diagnosis.

On the contrary, the blood density ensures the high visibility of the ulceration above the epidermis. Considered that the ulceration is a result of the uncontrollable proliferation of neoplastic cells due to expansive activity of the tumor, this aspect is an important marker for tumor manifestation.

To support this thesis, a wide inflammatory process lays below the ulceration, causing even the destruction of the epidermis in some parts which are visible only in the SR image (Fig. 3.b). The thickness of melanoma lesion, which is one of the fundamental parameters for evaluation of staging, is easily assessable even at this level of magnification.

B. X-ray virtual histology with SR micro-CT

By exploiting the propagation-based characteristics of the synchrotron setup, the high-contrast SR micro-CT allows to enhance soft tissue properties making easier to detect morphological and pathological aspects on a microscopic scale. As shown in Fig. 3.b, the SR micro-CT image categorizes skin layers in different shades of gray: the epidermis is the outer layer in dark gray, while dermis is the fibrous part in light gray, and subcutaneous adipose tissue is of a dense dark gray.

In Fig. 3.f it can be noticed that histology fails to appreciate the subcutaneous fat, which appears as background. Due to its weak structure, it is easily damageable by undergoing the mechanical compression of sectioning causing tears and rips in the histological tissue.

By virtually sectioning the 3D micro-CT dataset, the chosen slice in Fig. 3.d testifies the absence of an intact epidermis and the association between consumption of epidermis and ulceration [13]. Failing to recognize this could decrease the degree of severity and thus lead to a less rigorous prognosis [14]. However, an experienced pathologist can predict and capture the full-thickness loss of epidermis overlying melanoma by evaluating the infiltration of the epidermis by malignant melanocytes in the histological section. This fundamental aspect for staging, diagnosis and prognosis cannot be solved by SR micro-CT image due to its spatial resolution.

A great inflammation under the ulceration as in Fig. 3.b is a clear symptom of cancerogenesis, but it is difficult to differentiate malignant melanocytes from lymphocytes.

However, xVH provides good contrast to enhance high dense material giving complementary morphological information to the histology technique which highlight cells' nuclei in purple.

For this purpose, Fig. 3.g shows the structure of stratum basale, which is a single layer of basal cells, visible as a purple bow in the histological image and as a light gray coloured bow in the micro-CT one. Then, clusters of melanoma cells are observable as purple and gray nests in histology, while they appear as dark gray regions bounded by a white membrane in the micro-CT image. Melanin pigment is also visible in both images and even in Fig. 3.e as brownish elements in the histology image, and as white dots in the micro-CT one.

However, these aspects cannot be investigated by lab-based micro-CT which cannot reach a similar spatial resolution. Further improvements are needed to increase the visibility of tissue components at the microscopic scale.

C. X-ray virtual histology quantitative analysis

Table I reports the quantitative results obtained for the two micro-CT techniques.

TABLE I: RESULTS OF THE QUANTITATIVE ANALYSIS

Tissue element	*CNR Lab-based micro-CT*	*CNR SR micro-CT*
Ulceration	7.28	8.92
Lesion	2.10	1.30
Epidermis	2.41	1.13
Dermis	5.40	2.02
Subcutaneous fat	0.30	1.86

All results from both techniques are above the unity with only one exception, thus meaning an overall good visibility of the tissue. For both techniques, ulceration and dermis tend to have the highest CNR due to their high densities, while the lesion does not have a high CNR value due to its non-uniform composition. Due to the noisy paraffin background used as reference, lab-based technique reveals higher CNR values than SR ones, but this does not imply higher image definition. Consequently, the lowest CNR measure for lab-based method comes for subcutaneous fat because of the similar noisy pattern as the reference background.

IV. CONCLUSION

A suspected melanoma excised tissue was examined by histology and measured with two different micro-CT setups. While the SR micro-CT technique reaches a very high-resolution comparable to that achievable via large magnification in conventional histology, the compact phase-contrast lab-based micro-CT technique shows promising results when considering its use to assess the correct malignancy of the suspected melanoma. In addition, the computed quantitative measurements support the need of phase-contrast while performing xVH in both scenarios (synchrotron and laboratory) instead of conventional absorption X-ray scanning.

The proposed phase-contrast laboratory micro-CT cannot reach the performances of the considered SR micro-CT setup, due to the limited spatial resolution and low scanning speed, but still provides a comprehensive understanding of morphological and functional aspects of the melanoma tissue in a non-destructive way. Once fully operating and optimized, the inclusion of a lab-based micro-CT setup in a clinical context would help to provide information about the pathological stage of the disease.

ACKNOWLEDGEMENT

Authors acknowledge Elettra-Sincrotrone Trieste S.C.p.A. for providing access to the synchrotron radiation facility and for using SYRMEP beamline. This work is carried out in the framework of the PEPI project, supported by Istituto Nazionale di Fisica Nucleare (National Scientific Commission 5 for Technological and Inter-disciplinary Research, No. 22260/2020).

REFERENCES

[1] N. H. Matthews, W.-Q. Li, A. A. Qureshi, M. A. Weinstock, and E. Cho, 'Epidemiology of Melanoma', in *Cutaneous Melanoma: Etiology and Therapy*, W. H. Ward and J. M. Farma, Eds., Brisbane (AU): Codon Publications, 2017. Accessed: Oct. 18, 2022. [Online]. Available: http://www.ncbi.nlm.nih.gov/books/NBK481862/

[2] M.-F. Demierre, 'Epidemiology and prevention of cutaneous melanoma', *Curr. Treat. Options Oncol.*, vol. 7, no. 3, pp. 181–186, May 2006, doi: 10.1007/s11864-006-0011-z.

[3] K. H. Kaidbey, P. P. Agin, R. M. Sayre, and A. M. Kligman, 'Photoprotection by melanin--a comparison of black and Caucasian skin', *J. Am. Acad. Dermatol.*, vol. 1, no. 3, pp. 249–260, Sep. 1979, doi: 10.1016/s0190-9622(79)70018-1.

[4] K. Kratkiewicz *et al.*, 'Photoacoustic/Ultrasound/Optical Coherence Tomography Evaluation of Melanoma Lesion and Healthy Skin in a Swine Model', *Sensors*, vol. 19, no. 12, p. 2815, Jun. 2019, doi: 10.3390/s19122815.

[5] L. Brombal, F. Arfelli, R. H. Menk, L. Rigon, and F. Brun, 'PEPI Lab: a flexible compact multi-modal setup for X-ray phase-contrast and spectral imaging', *Sci. Rep.*, vol. 13, no. 1, Art. no. 1, Mar. 2023, doi: 10.1038/s41598-023-30316-5.

[6] R. Bellazzini *et al.*, 'PIXIE III: a very large area photon-counting CMOS pixel ASIC for sharp X-ray spectral imaging', *J. Instrum.*, vol. 10, no. 01, p. C01032, Jan. 2015, doi: 10.1088/1748-0221/10/01/C01032.

[7] A. Biguri, M. Dosanjh, S. Hancock, and M. Soleimani, 'TIGRE: a MATLAB-GPU toolbox for CBCT image reconstruction', *Biomed. Phys. Eng. Express*, vol. 2, no. 5, p. 055010, Sep. 2016, doi: 10.1088/2057-1976/2/5/055010.

[8] A. A. Hendriksen, D. M. Pelt, and K. J. Batenburg, 'Noise2Inverse: Self-Supervised Deep Convolutional Denoising for Tomography', *IEEE Trans. Comput. Imaging*, vol. 6, pp. 1320–1335, 2020, doi: 10.1109/TCI.2020.3019647.

[9] G. Tromba *et al.*, 'The SYRMEP Beamline of Elettra: Clinical Mammography and Bio-medical Applications', *AIP Conf. Proc.*, vol. 1266, no. 1, pp. 18–23, Jul. 2010, doi: 10.1063/1.3478190.

[10] S. Donato *et al.*, 'Optimization of a customized simultaneous algebraic reconstruction technique algorithm for phase-contrast breast computed tomography', *Phys. Med. Biol.*, vol. 67, no. 9, p. 095012, Apr. 2022, doi: 10.1088/1361-6560/ac65d4.

[11] D. Paganin, S. C. Mayo, T. E. Gureyev, P. R. Miller, and S. W. Wilkins, 'Simultaneous phase and amplitude extraction from a single defocused image of a homogeneous object', *J. Microsc.*, vol. 206, no. 1, pp. 33–40, 2002, doi: 10.1046/j.1365-2818.2002.01010.x.

[12] F. Brun *et al.*, 'SYRMEP Tomo Project: a graphical user interface for customizing CT reconstruction workflows', *Adv. Struct. Chem. Imaging*, vol. 3, no. 1, p. 4, 2017, doi: 10.1186/s40679-016-0036-8.

[13] R. F. Walters *et al.*, 'Consumption of the epidermis: a criterion in the differential diagnosis of melanoma and dysplastic nevi that is associated with increasing breslow depth and ulceration', *Am. J. Dermatopathol.*, vol. 29, no. 6, pp. 527–533, Dec. 2007, doi: 10.1097/DAD.0b013e318156e0a7.

[14] M. L. Bønnelykke-Behrndtz and T. Steiniche, 'Ulcerated Melanoma: Aspects and Prognostic Impact', in *Cutaneous Melanoma: Etiology and Therapy*, W. H. Ward and J. M. Farma, Eds., Brisbane (AU): Codon Publications, 2017. Accessed: Dec. 20, 2022. [Online]. Available: http://www.ncbi.nlm.nih.gov/books/NBK481861/